Propensity of Soft Ions for the Air/Water Interface

Luboš Vrbka, Martin Mucha, Babak Minofar, and Pavel Jungwirth*

Institute of Organic Chemistry and Biochemistry, Academy of Sciences of the Czech Republic, and Center for Complex Molecular Systems and Biomolecules, Flemingovo nam. 2, 16610 Prague 6, Czech Republic

Eric C. Brown and Douglas J. Tobias*

Department of Chemistry and Institute for Surface and Interface Science, University of California, Irvine, CA 92697-2025, USA

***To whom correspondence should be addressed. P. J. :e-mail: pavel.jungwirth@uochb.cas.cz, phone: ++420-220410314, FAX: ++420-220410320. D. J. T.: e-mail: dtobias@uci.edu, phone: ++1-9498244295, FAX: ++1-9498248571.**

Major recent advances

Results of molecular dynamics simulations with polarizable force fields, supported by surface sensitive experiments, indicate that the propensity of atomic and hydrophilic molecular ions for the air/water interface exhibits strong ion specificity. While hard, non-polarizable ions are repelled from the interface, soft, polarizable ions exhibit surface affinity.

Introduction

The studies of surface properties of simple electrolytes date back to early 1900s, when Adolf Heydweiller performed surface tension measurements for a series of aqueous salt solutions[1]. The main findings were as follows: i) adding simple salts raises surface tension of water, ii) for cations there is little ion specificity, while iii) the effect of anions is specific and follows the Hofmeister series[2], with strongly hydrated anions raising surface tension more than weakly hydrated ones. In the 1930s this effect was semi-quantitatively rationalized by Onsager and Samaras[3] via the Gibbs equation[4] in terms of repulsion of ions from the air/water interface by electrostatic image forces. It has since become a common wisdom that surfaces of aqueous solutions of simple salts are formed by an ion-free water layer[5].

The first indication that the above picture is not entirely correct came from cluster studies in the 1990s. Both photoelectron experiments[6,7] and molecular dynamics simulations[8-10] showed ion specificity in the behavior of alkali cations and halide anions in water clusters. While alkali cations and fluoride solvate inside medium sized clusters (with roughly 10-100 water molecules), heavier halides tend to solvate asymmetrically, i.e., to reside on the surface of the cluster. Molecular dynamics simulations showed that this ion specificity is due to the ion polarity, size, and, in particular, polarizability. A theoretical study by Stuart and Berne[11] indicated that for

chloride the surface effect is primarily due to the finite size and surface curvature of the water cluster. It was, therefore, unclear whether the cluster results can be directly extrapolated to extended, flat surfaces. Note, that for aqueous salt droplets with a diameter larger than roughly 1 μm curvature effects become negligible and, consequently, their surface can be viewed as flat. Such particles are ubiquitous, e.g., in the atmosphere (aqueous sea salt aerosols) and their molecular structure and reactivity has been intensely studied recently[12-14]. In the following we summarize results of molecular dynamics simulations of extended interfaces between air and aqueous solutions of simple salts.

Soft Ions at the Air/Water Interface

A well established procedure exists for performing molecular dynamics simulations of extended slabs, possessing a liquid bulk region in between two flat air/water interfaces[15]. One simply employs periodic boundary conditions with a unit cell with one dimension significantly elongated. In a typical simulation, an orthogonal unit cell with dimensions 3x3x10 nm is used, containing a slab of ~900 water molecules and a specific amount of salt ions[16]. Note that under normal atmospheric pressure less than a single molecule of nitrogen is on average present in the void above or below the aqueous slab. Therefore, for the purpose of the present discussion we can interchangeably use the terms vacuum/water and air/water interfaces.

Early molecular dynamics simulations of slabs containing aqueous NaCl solutions employing a non-polarizable force field showed a certain degree of ion specificity[15]. Namely, chloride penetrated closer to the surface than sodium, however, both ions were effectively repelled from the interface. The surface effects and ion specificity become much more pronounced upon using a polarizable force field[17,18]. This is clearly demonstrated in the

composite Fig. 1, which depicts results from molecular dynamics simulations of a series of slabs of 1.2 M aqueous sodium halides. The left and middle columns show top and side views of typical snapshots from the simulations. The right column depicts statistically averaged density profiles of cations, anions, and water oxygens, histogrammed in thin slices parallel with the interface. The water oxygen signal defines the slab extensions, with a constant value (normalized to one) corresponding to the aqueous bulk and the decrease to zero within ~0.4 nm to the interfacial region.

We see from the top pair of pictures that sodium and fluoride behave in our molecular simulations in accord with the traditional continuum dielectric boundary picture[3,5,19], which invokes repulsion from the air/water interface by image forces. However, the situation is very different for heavier halides, with the chloride ions moving all the way to the interface, and bromide and iodide even exhibiting a peak in density at the surface. Note that for the latter two ions accumulation at the surface is accompanied by depletion from the subsurface layer where, as a matter of fact, the sodium cations exhibit a peak in density. As a result, an electric potential develops at the interface with a sign and magnitude correlating with earlier experimental results[5]. In addition, the values of surface tension, which are directly related to the asymmetry of the pressure tensor, have been extracted from the simulations. It is very encouraging that the molecular dynamics simulations succeeded to semi-quantitatively recover the experimental surface tension increase $\Delta\gamma$ with respect to pure water for the whole sodium halide series, including the Hofmeister ordering $\Delta\gamma(F^-) > \Delta\gamma(Cl^-) > \Delta\gamma(Br^-) > \Delta\gamma(I^-)$[17].

Although the propensity of soft, polarizable anions for the air-water interface is a complicated function of ionic size, polarity, and polarizability, simulations performed with polarizable and non-polarizable force fields clearly show that it is the last parameter which to the

largest extent determines this effect[13,16]. Fig. 2 schematically shows a polarizable atomic anion in the aqueous bulk and at the air/water interface. In the liquid bulk, water molecules arrange roughly symmetrically around the ion. As a result, the vectorial sum of the dipoles of these water molecules is very small (zero on average). The situation is very different at the interface where, schematically, water molecules are present only on one side of the ion. Consequently, there is a significant electric field resulting from the sum of water dipoles polarizing the soft anion. This leads to an additional stabilization at the interface which can, for sufficiently polarizable ions, overwhelm the loss of ion-water electrostatic interactions.

In reality, the picture is more complex than the schematic Figure 2. The aqueous interface is not perfectly flat but rather corrugated and the water structure around the ion is thermally disordered. Moreover, water polarizability comes into play, too; not only water dipoles polarize the soft anion but also the ion polarizes water in a complex, non-additive fashion. To explore these effects in detail we performed a series of four simulations of aqueous slabs containing 1.2 M of sodium iodide. In the first simulation, the results of which are depicted in Fig. 3a, a non-polarizable force field was employed. We see from the density profiles that in this case both sodium and iodide ions are repelled from the air/water interface. Still, there is a weak specificity due to ion size and polarity, which results in the iodide signal being shifted closer to the surface than that of sodium. Fig. 3b shows density profiles from a simulation with non-polarizable ions but polarizable water. Including water polarizability results in iodide moving closer to the interface, exhibiting a sizable surface peak and subsurface depletion. Upon performing a simulation with polarizable ions in non-polarizable water (see Fig. 3c), the propensity of iodide for the air/water interface becomes stronger than in the previous case, and the sodium ions start to exhibit a subsurface peak. The combined effect of polarizable ions and water[17], as depicted in

Fig. 3d, leads to the strongest surface enhancement (by up to a factor of three) of iodide concentration, with subsurface depletion close to the region where the sodium concentration peaks.

The densities presented in Fig. 3 clearly demonstrate that anion polarizability is an important factor in determining the propensity of an ion for the air-water interface. However, as one moves down the series of halides (F^-, Cl^-, Br^-, I^-), the size of the ion increases along with the polarizability, and it is conceivable that ion size could also play a role in determining adsorption propensity. To test this hypothesis, we have carried out a simulation of a 1.2 M solution of the sodium salt of a hybrid anion that has the size of iodide but the polarizability of chloride, in polarizable water. The simulations were performed with a unit box containing roughly twice as many atoms as in the previous case, in order to explore also the possible effect of the thickness of the slab. The density profile of the hybrid anion is compared to those of polarizable iodide and chloride in Fig. 4. In contrast to the chloride density, which approaches the Gibbs dividing surface but does not exhibit a peak in the interfacial region, the hybrid anion does exhibit a peak, suggesting surfactant activity, albeit not as strongly as iodide. Thus, for the determination of the interfacial propensity of the halide ions, size matters as well as polarizability. In addition, the effect of water polarizability is non-negligible (compare Figs. 3b and 4).

The polarizability driven surface propensity is not limited to atomic anions. We have investigated the interfacial behavior of three atmospherically relevant hydrophilic molecular anions: nitrate[20], sulfate[21], and bisulfate. The polarizability of nitrate, albeit anisotropic, is roughly of the same mean value as that of bromide. Consequently, NO_3^- exhibits a very similar propensity for the air/water interface as Br^-. Sulfate is even more polarizable than nitrate with

polarizability in water (note that SO_4^{2-} does not exist in the gas phase due to a spontaneous electron detachment[22]) equal to 7.1 A^3. Nevertheless, molecular dynamics simulations show that sulfate is repelled from the air/water interface and prefers bulk solvation, in agreement with photoelectron experiments in large aqueous clusters[22-24]. This is due to the multiple charge, which shifts the balance from "surface-driving" polarization interactions to "bulk-driving" electrostatic forces. Finally, our most recent simulations show that the rather polarizable monovalent HSO_4^- ion with a strongly hydrophilic OH group turns out to be an intermediate case between bulk and interfacial solvation, behaving similar to chloride.

The force that drives polarizable atomic and hydrophilic molecular ions to the air/water interface is qualitatively different from that acting on hydrophobic ionic surfactants. This is nicely demonstrated on Fig. 5, which depicts our recent results of polarizable and non-polarizable simulations of a single tetra-butyl ammonium iodide ion pair in an aqueous slab. Each of the two ions was initially placed on one of the two air/water interfaces of an aqueous slab. Within a simulation employing a polarizable force field both ions exhibit surfactant activity and remain at the interface (see Fig. 5a). The behavior of the tetra-butyl ammonium cation does not change significantly upon switching off polarizability. This is due to the fact that the hydrophobic interactions of the alkyl chains dominate. However, as shown in Fig. 5b, a non-polarizable iodide moves from the interface into the aqueous bulk, demonstrating again that its surface affinity is primarily due to polarization interactions.

Consistency with Experimental Observations

The traditional view of an ion-free interface was based largely on analysis of the surface tension of aqueous solutions using the Gibbs adsorption isotherm[25]:

$$d\gamma = -\Gamma d\mu. \tag{1}$$

Here γ is the surface tension, μ is the chemical potential of the solute, and Γ is the surface excess of the solute:

$$\Gamma = \frac{1}{A}\left(n_{total} - n_{liq} - n_{gas}\right), \tag{2}$$

where A is the surface area of the interface, n_{total} is the total number of moles of solute, and n_{liq} and n_{gas} are the moles of solute in the liquid and gas phases, respectively. Note that equation (1) assumes that there is a single solute, and that the interface is defined by the Gibbs dividing surface, for which the surface excess of the solvent vanishes. Inserting $d\mu = -RTd\,ln\,a$ into equation (1) and rearranging, we obtain:

$$\left(\frac{d\gamma}{d\,ln\,a}\right)_T = -RT\Gamma, \tag{3}$$

where a is the solute activity. Thus, the observed increase of the surface tension with the activity (concentration) of many inorganic salts, including the alkali halides[5], corresponds to a negative surface excess of ions.

Our simulations suggest that there are two ways to get a negative Gibbs surface excess. To illustrate this, we rewrite the definition (equation (2)) in terms of an ion density profile, $\rho(z)$:

$$\Gamma = \int_{-\infty}^{\infty} \rho(z)dz - \rho_{liq}\int_{z_{Gibbs}}^{\infty} dz - \rho_{gas}\int_{0}^{z_{Gibbs}} dz, \tag{4}$$

where ρ_{liq} and ρ_{gas} are the (constant) densities in the bulk liquid and gas phases, respectively. Noting that for ions, $\rho_{gas} = 0$, we can rearrange equation (4) to

$$\Gamma = \int_{0}^{z_{Gibbs}} \rho(z)dz + \int_{z_{Gibbs}}^{\infty} \left[\rho(z) - \rho_{liq}\right]dz. \tag{5}$$

This equation is the basis of a graphical demonstration in Fig. 6 of two scenarios that can give rise to $\Gamma < 0$ (since atomic cations are repelled from the interface in accord with the traditional

view, here we limit the discussion to the more complex case of atomic anions). Fig. 6 (top) depicts the scenario embodied in the traditional view, where anions are repelled from the interface, as exemplified by F^-. Fig. 6 (bottom) depicts the case of the heavier halide salts, e.g. NaBr and NaI, where there is a density enhancement at the surface followed by a depletion in the subsurface region (i.e., an oscillatory density profile). Note that, as long as the depletion is greater than the enhancement, the thermodynamic surface excess is negative. Thus, an increase of surface tension with solute concentration does not rule out the presence of a solute at the interface, and care should be taken when interpreting surface tension data on aqueous electrolyte solutions.

Two well-established experimental techniques for directly probing structure in the inhomogeneous interfacial region of liquid surfaces have recently had mixed success at detecting the presence of ions at the air-water interface. One is specular X-ray reflectometry (XRR)[26], which probes electron density distributions in the direction normal to the surface. In collaboration with experimental colleagues, we recently attempted to use synchrotron XRR to detect the pronounced enhancement of electron density expected at the air-solution interface of aqueous alkali iodides according to the predictions of our simulations (see Fig. 3d). Within experimental uncertainty the reflectivity data for neat water and the alkali iodide salt solutions were indistinguishable, and at first glance this seems to cast doubt on the predicted surface enhancement of iodide anions. However, a plausible explanation is that the surface roughness due to long-wavelength capillary waves (which are not present in the relatively small systems we simulate) wash out the enhancement of electron density due to ion adsorption. This was confirmed by computing reflectivities from the electron density profiles obtained from our

simulations, including the roughness due to capillary waves (by Gaussian smoothing using widths extracted from experimental data).

In another set of experiments, Liu et al.[27] used vibrational sum frequency generation (VSFG) to investigate aqueous sodium halide solutions. VSFG is an interface-selective vibrational spectroscopy, which in the application cited focused on probing the water OH stretch, and hence provided information on changes in interfacial water structure upon addition of sodium halide salts. The VSFG data of Liu et al.[27] appear to be essentially consistent with our MD simulations: the spectra for NaF and NaCl solutions are similar to the neat water spectrum, suggesting negligible perturbations of the water structure in the interfacial region, while the spectra of NaBr and NaI solutions suggest significant perturbations of the hydrogen bonding in the interfacial region that increase with increasing concentration. Moreover, a comparison of the SFG data to infrared and Raman spectra obtained in the same study indicates an increase in the width of the interface of NaBr and NaI solutions compared to neat water, consistent with the predictions of our simulations (c.f. Fig. 1).

Conclusions

Recent molecular dynamics simulations of slabs of aqueous salt solutions indicate a strong specificity in the propensity of the solvated atomic and small hydrophilic molecular ions for the air/water interface. Small hard (non-polarizable) ions, such as alkali cations or fluoride, are repelled from the surface in accord with the standard Onsager-Samaras theory. However, large soft (polarizable) ions, such as heavier halides or nitrate, exhibit an affinity for the air/water interface. Although the propensity of soft anions for the interface depends on several factors, the

main driving forces for are the stabilizing polarization interactions in the anisotropic environment of the interface.

Acknowledgements

Support from the Czech Ministry of Education (grant No. ME644) and the US National Science Foundation (grant CHE-0209719) is gratefully acknowledged. We thank Prof. John A. Wheeler for helpful discussions on the Gibbs surface excess, and Prof. Mathias Lösche and Dr. Peter Krueger for performing the X-ray reflectivity experiments.

Figure Captions

Fig. 1 Left and middle columns: top and side views of snapshots of solution/air interfaces from MD simulations of 1.2 M sodium halide solutions. Right: corresponding number density profiles. Coloring scheme: water oxygen, blue; water hydrogen, gray; sodium ions, green; chloride ions, yellow; bromide ions, orange; iodide ions, magenta.

Fig. 2 A schematic picture of interactions between a polarizable anion and water molecules a) in the aqueous bulk, and b) at the air/water interface.

Fig. 3 Density profiles of water oxygen (blue), sodium (green), and iodide (red) from the center to the surface of a 1.2 M aqueous NaI slab. a) Non-polarizable force field, b) non-polarizable ions and polarizable water, c) polarizable ions and non-polarizable water, and d) polarizable force field.

Fig. 4 Density profiles of water oxygen (blue), iodide with its natural polarizability (red), iodide with the polarizability of chloride (brown), and chloride with its natural polarizability (violet) from the center to the surface of a 1.2 M aqueous sodium halide solution.

Fig. 5 Density profiles of tetra-butyl ammonium cation (nitrogen - green) and iodide (black) across the whole water slab (oxygen – red). a) Polarizable force field, and b) non-polarizable force field.

Fig. 6 Schematic depiction of the determination of the Gibbs surface excess from ion density profiles. Top: case of ion repulsion from the interface (e.g. F^-), bottom: case of inhomogeneous ion density profile with a surfactant layer and depletion zone (e.g. Br^-, I^-). The areas shaded green give negative contributions to the Gibbs surface excess, and the red gives a positive contribution (see text).

Figure 1

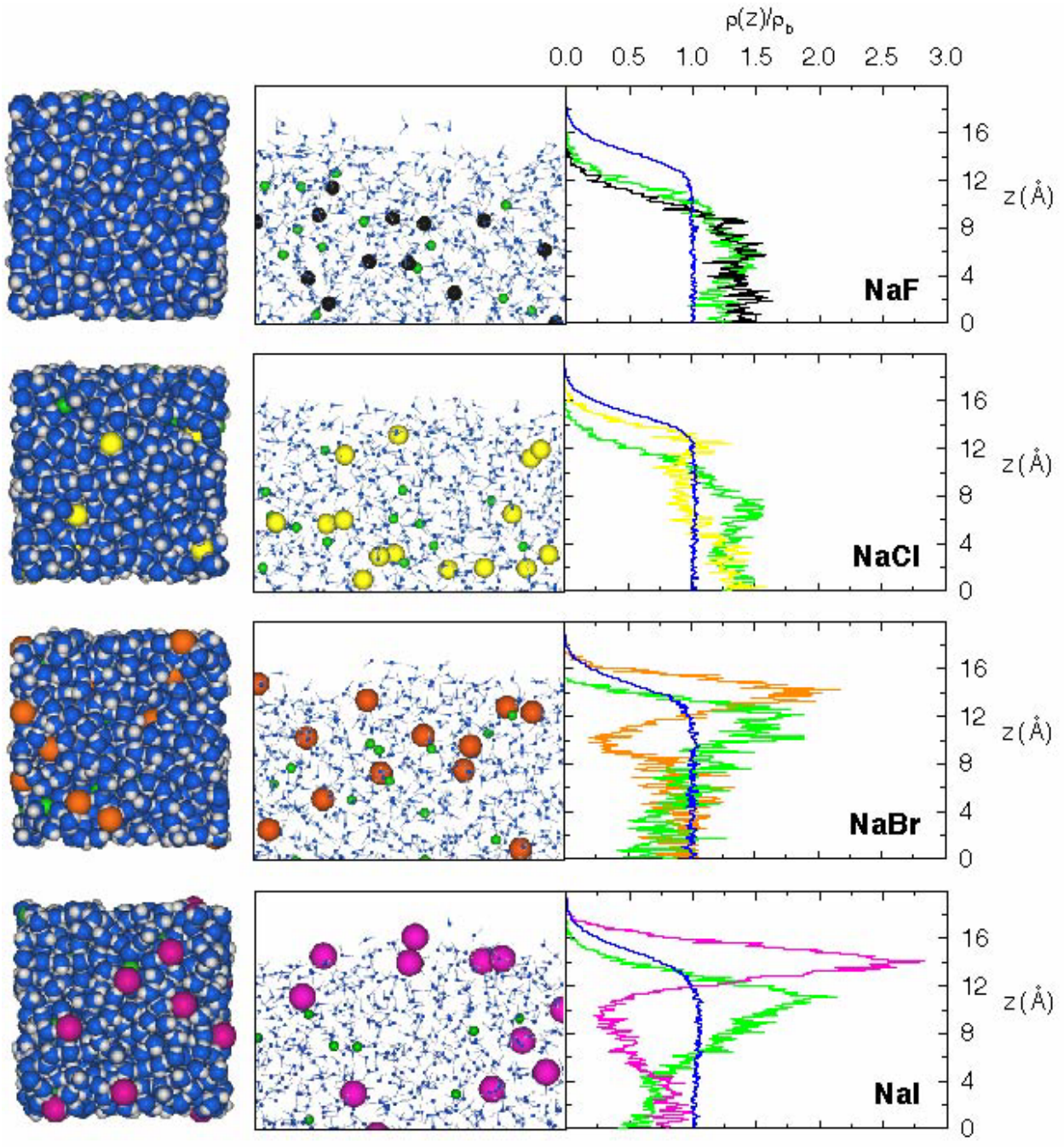

Figure 2a

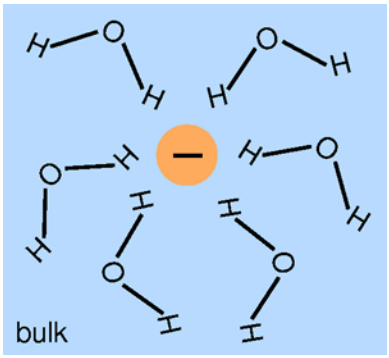

Figure 2b

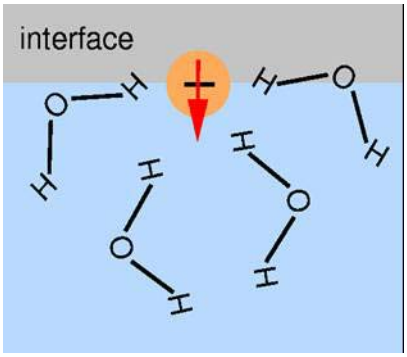

Figure 3a

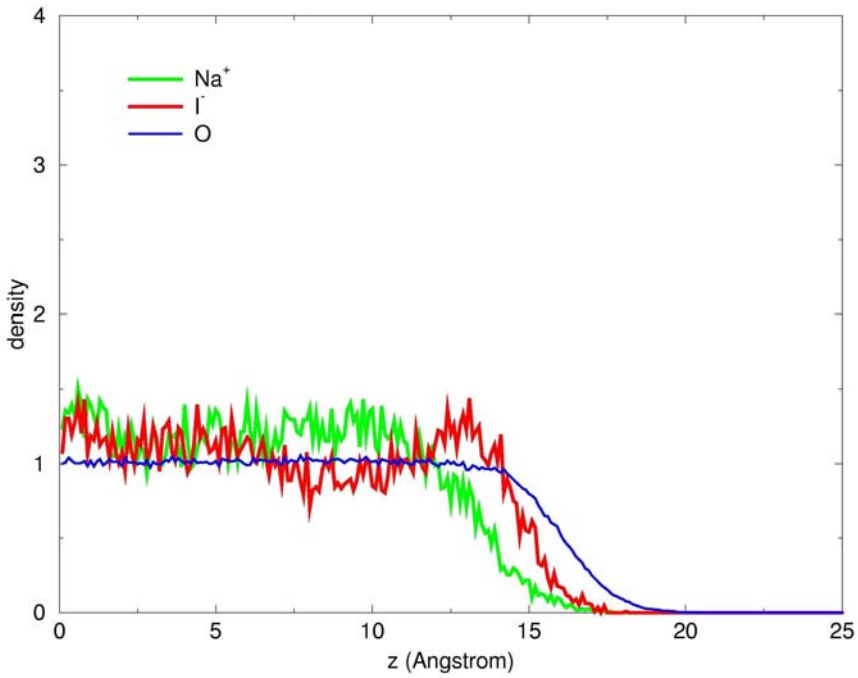

Figure 3b

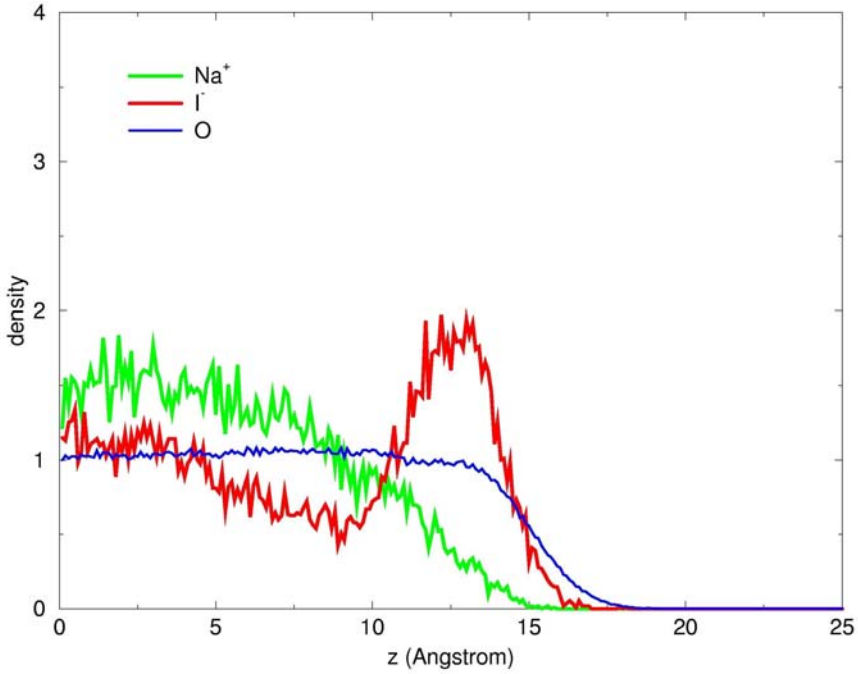

Figure 3c

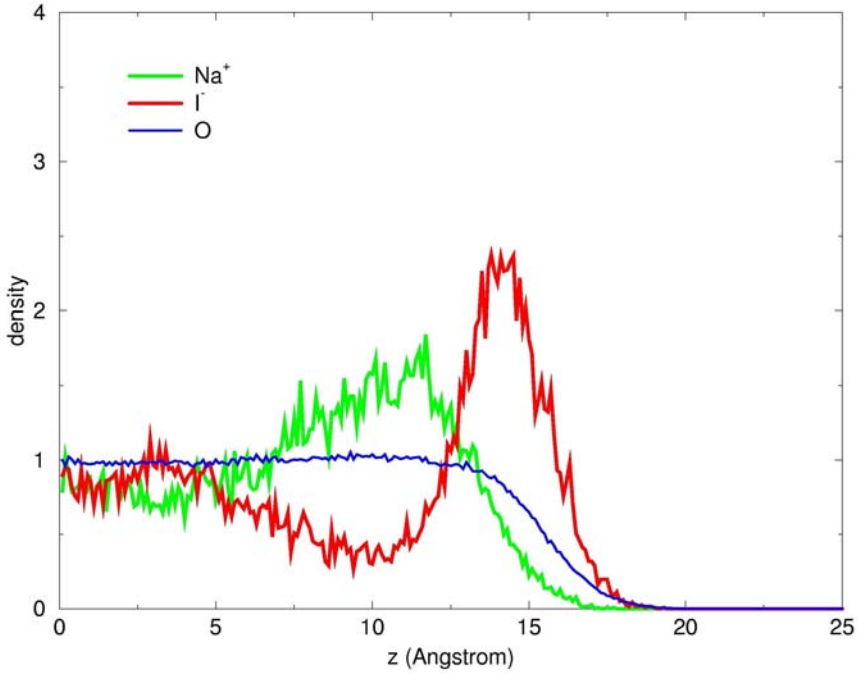

Figure 3d

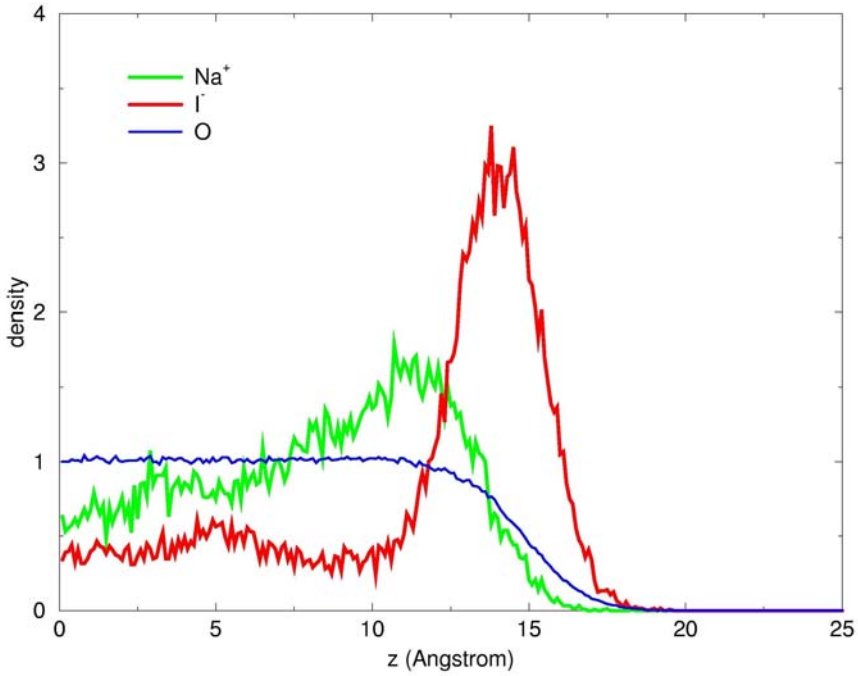

Figure 4

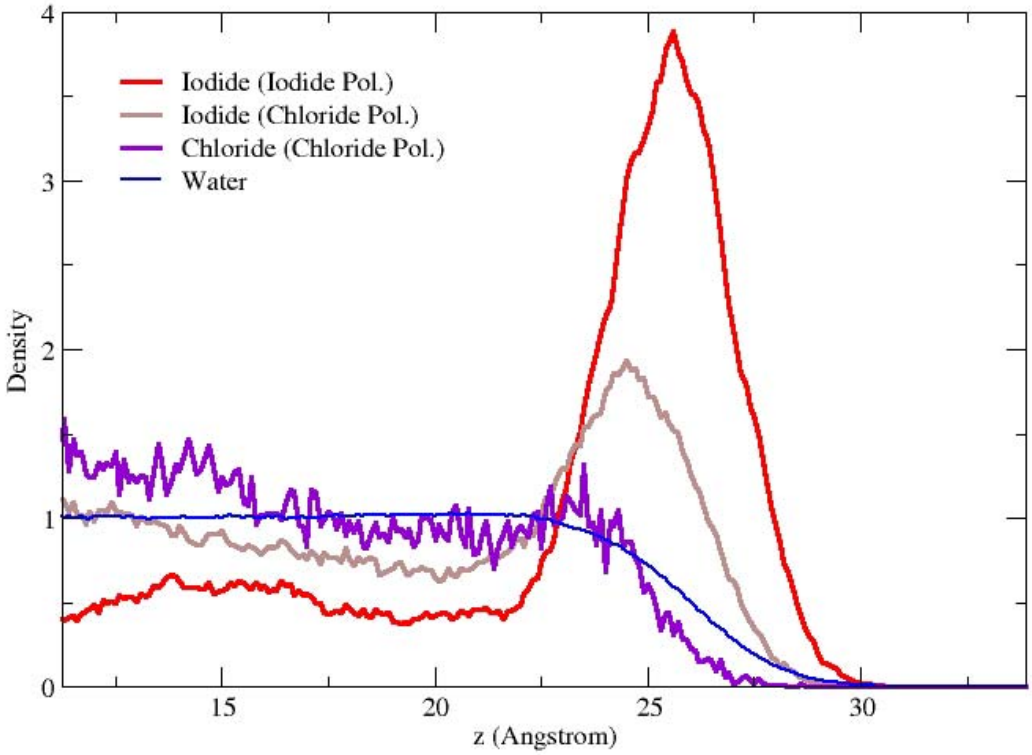
Iodide (Iodide Pol.)
Iodide (Chloride Pol.)
Chloride (Chloride Pol.)
Water
Density
z (Angstrom)
0
1
2
3
4
15
20
25
30

Figure 5a

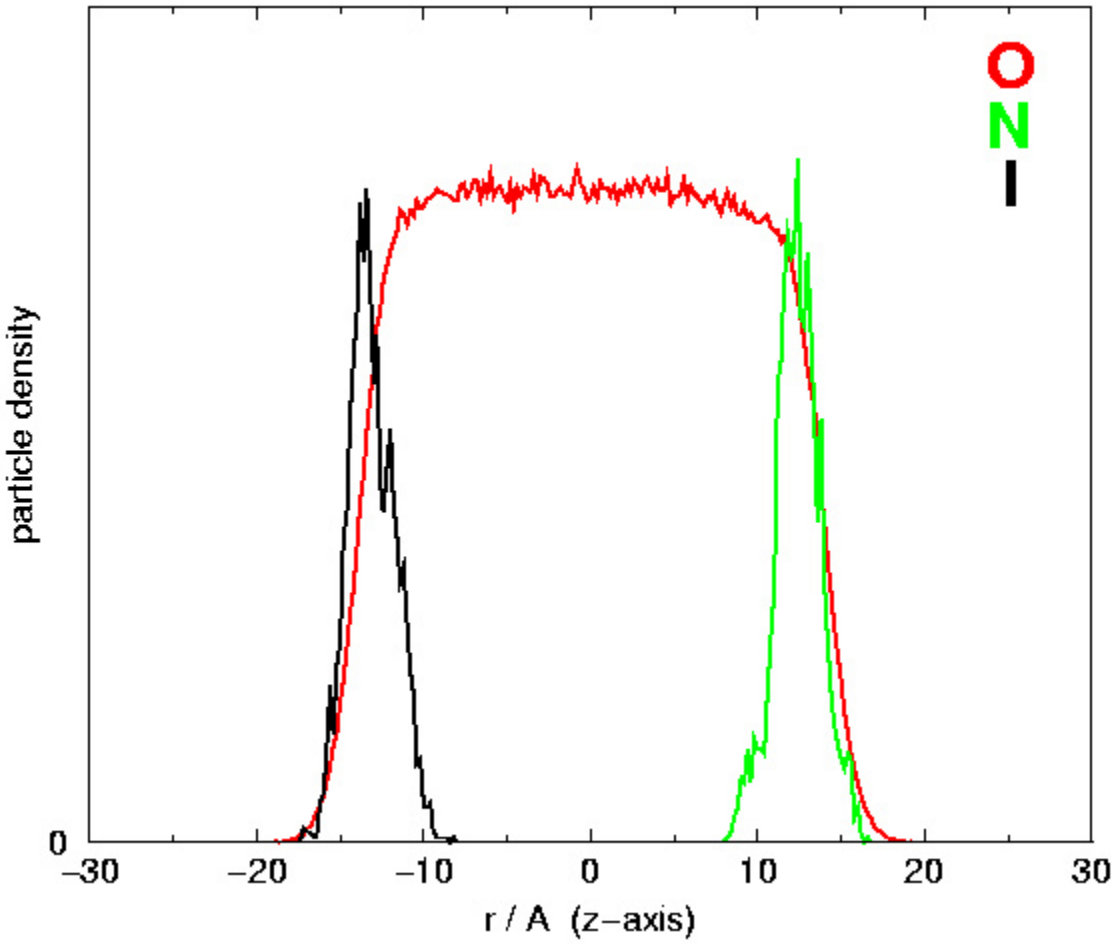

Figure 5b

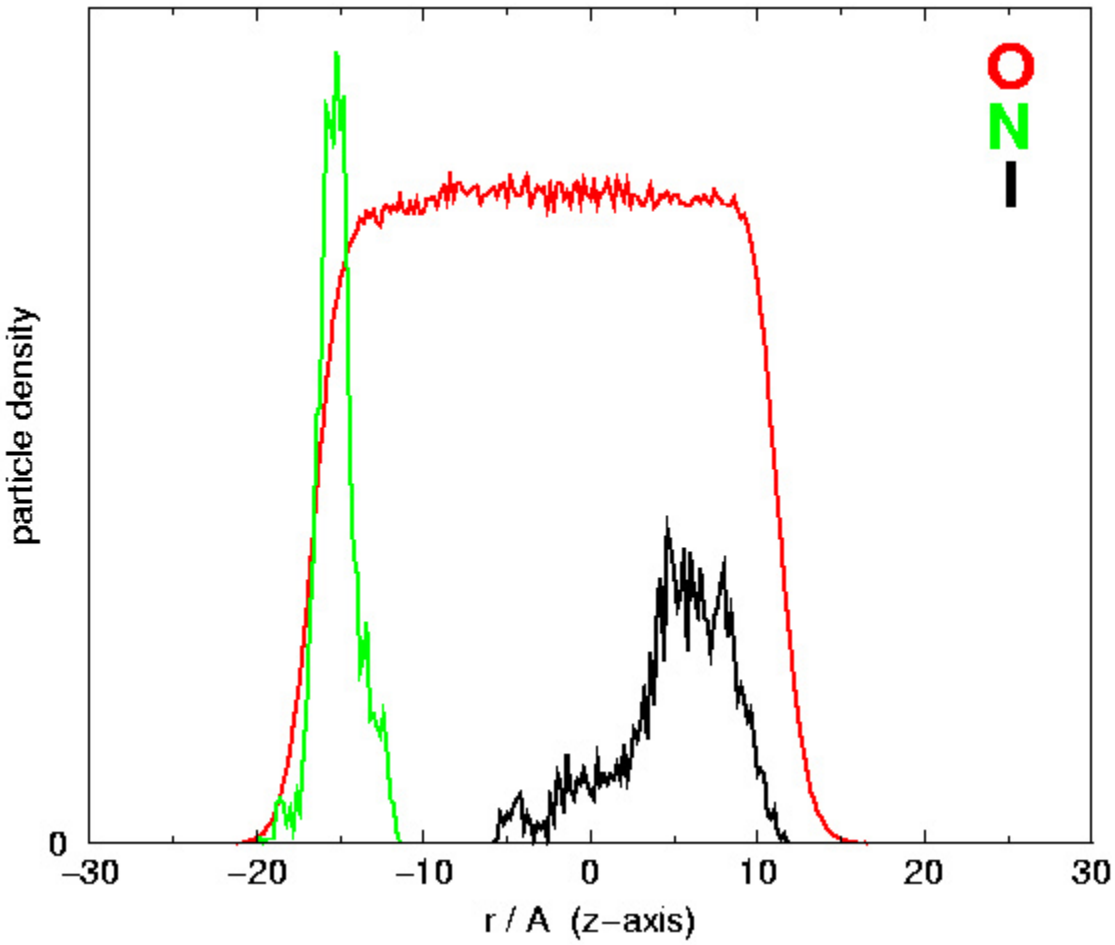

Figure 6

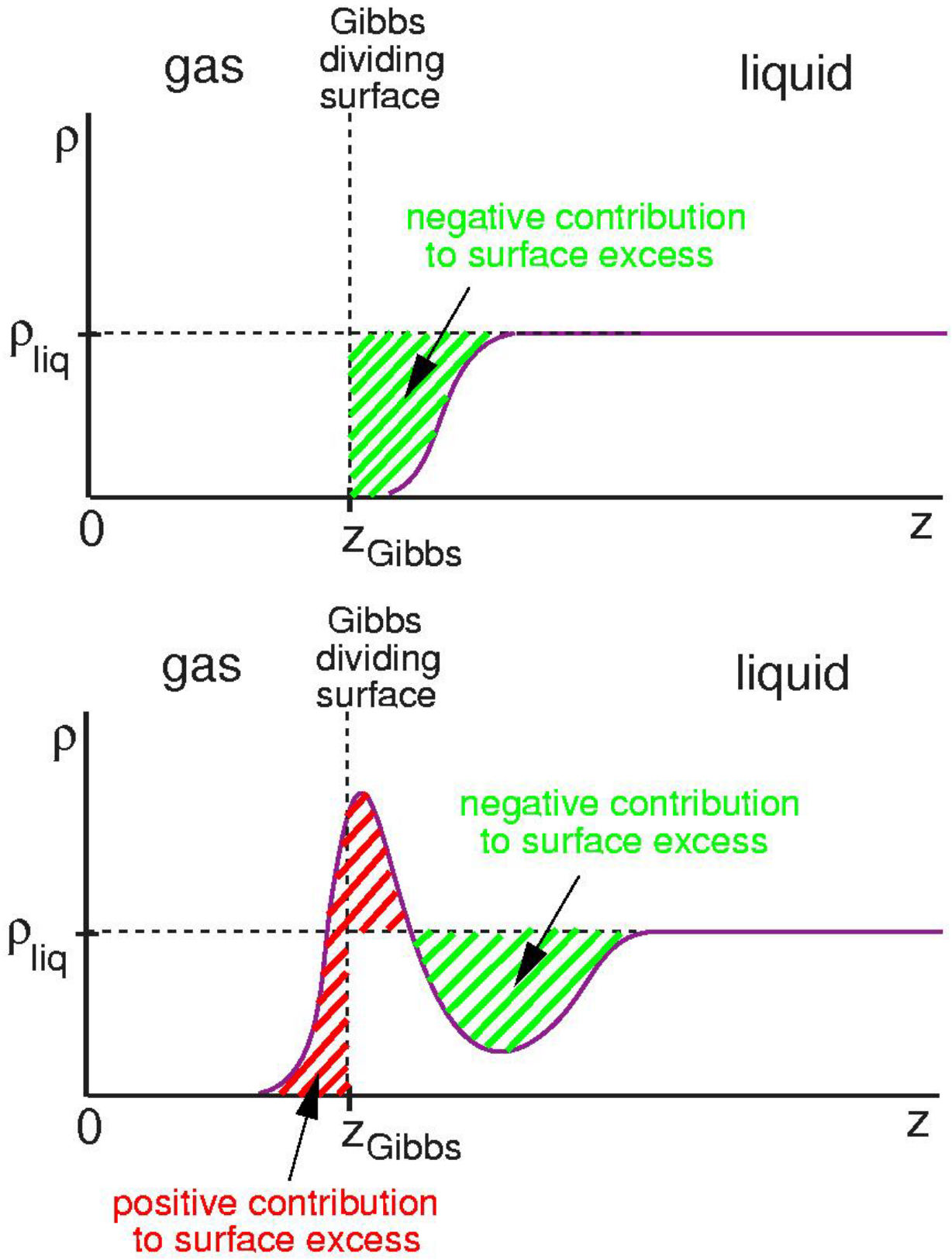
gas
Gibbs dividing surface
liquid
ρ
negative contribution to surface excess
ρliq
0
zGibbs
z
gas
Gibbs dividing surface
liquid
ρ
negative contribution to surface excess
ρliq
0
zGibbs
z
positive contribution to surface excess

References

(1) Heydweiller, A. *Ann. Physik.* **1910**, *33*, 145.

(2) Hofmeister, F. *Arch. Exp. Pathol. Pharmakol. (Leipzig)* **1888**, *24*, 247.

(3) Onsager, L.; Samaras, N. N. T. *J. Chem. Phys.* **1934**, *2*, 528.

(4) Gibbs, J. W. *The Collected Works of J. Willard Gibbs*; Longmans: New York, 1928.

(5) Randalls, J. E. B. *Phys. Chem. Liq.* **1977**, *7*, 107.

(6) Markovich, G.; Giniger, R.; Levin, M.; Cheshnovsky, O. *J. Chem. Phys.* **1991**, *95*, 9416.

(7) Markovich, G.; Pollack, S.; Giniger, R.; Cheshnovsky, O. *J. Chem. Phys.* **1994**, *101*, 9344.

(8) Perera, L.; Berkowitz, M. L. *J. Chem. Phys.* **1991**, *95*, 1954.

(9) Dang, L. X.; Smith, D. E. *J. Chem. Phys.* **1993**, *99*, 6950.

(10) Perera, L.; Berkowitz, M. L. *J. Chem. Phys.* **1994**, *100*, 3085.

(11) Stuart, S. J.; Berne, B. J. *J. Phys. Chem. A* **1999**, *103*, 10300.

(12) Oum, K. W.; Lakin, M. J.; DeHaan, D. O.; Brauers, T.; Finlayson-Pitts, B. J. *Science* **1998**, *279*, 74.

(13) Knipping, E. M.; Lakin, M. J.; Foster, K. L.; Jungwirth, P.; Tobias, D. J.; Gerber, R. B.; Dabdub, D.; Finlayson-Pitts, B. J. *Science* **2000**, *288*, 301.

(14) Laskin, A.; Gaspar, D. J.; Wang, W. H.; Hunt, S. W.; Cowin, J. P.; Colson, S. D.; Finlayson-Pitts, B. J. *Science* **2003**, *301*, 340.

(15) Benjamin, I. *J. Chem. Phys.* **1991**, *95*, 3698.

(16) Jungwirth, P.; Tobias, D. J. *J. Phys. Chem. B* **2002**, *106*, 6361.

(17) Jungwirth, P.; Tobias, D. J. *J. Phys. Chem. B* **2001**, *105*, 10468.

(18) Dang, L. X.; Chang, T. M. *J. Phys. Chem. B* **2002**, *106*, 235.

(19) Adam, N. K. *The Physics and Chemistry of Surfaces*; Oxford University Press: London, 1941.

(20) Salvador, P.; Curtis, J. E.; Tobias, D. J.; Jungwirth, P. *Phys. Chem. Chem. Phys.* **2003**, *5*, 3752.

(21) Jungwirth, P.; Curtis, J. E.; Tobias, D. J. *Chem. Phys. Lett.* **2003**, *367*, 704.

(22) Wang, X.-B.; Nicholas, J. B.; Wang, L.-S. *J. Chem. Phys.* **2000**, *113*, 10837.

(23) Wang, X.-B.; Yang, X.; Nicholas, J. B.; Wang, L.-S. *Science* **2001**, *294*, 1322.

(24) Yang, X.; Wang, X.-B.; Wang, L.-S. *J. Phys. Chem. A* **2002**, *106*, 7607.

(25) Defay, R.; Prigogine, I.; Bellemans, A. *Surface Tension and Adsorption*; Longmans Green: London, 1966.

(26) Alsnielsen, J.; Jacquemain, D.; Kjaer, K.; Leveiller, F.; Lahav, M.; Leiserowitz, L. *Physics Rep.* **1994**, *246*, 252.

(27) Liu, D. F.; Ma, G.; Levering, L. M.; Allen, H. C. *J. Phys. Chem. B* **2004**, *108*, 2252.